Significance of the South Pacific Convergence Zone in Energy Conversions of the Southern Hemisphere during FGGE, 10–27 January 1979

HUO-JIN HUANG* AND DAYTON G. VINCENT

Department of Geosciences, Purdue University, West Lafayette, IN 47907

(Manuscript received 16 July 1984, in final form 29 March 1985)

ABSTRACT

A modified set of Level III-b grid point analyses, originally produced by ECMWF, is used to diagnose the circulation features and energy conversions in the Southern Hemisphere during the FGGE SOP-1 period of 10–27 January 1979. One of the dominant features during the period was the South Pacific Convergence Zone (SPCZ), a large-scale, quasi-stationary, convectively-active cloud band over the South Pacific Ocean. The study focuses on the significance of the SPCZ on Southern Hemisphere energy conversions by partitioning the conversions into zonal and eddy (transient and standing) components. The mean state is examined for a 15-day period, 10–24 January, when the SPCZ was most active. After 24 January it dissipated. In addition, daily variations are examined for the entire period and a zonal wavenumber analysis for wavenumbers 1–15 is performed.

The major findings are that 1) the baroclinic conversion of eddy potential to eddy kinetic energy (*CE*) is the dominant conversion term in the tropics (0–30°S), and it is particularly important in the vicinity of the SPCZ; 2) all conversion terms in middle latitudes (30–60°S) are comparable and equally important; 3) standing (transient) eddies make the most significant contribution to *CE* (all eddy conversion terms) in the tropics and SPCZ area (midlatitudes); 4) wavenumber 4 dominates the *CE* conversion in the tropics, whereas wavenumbers 5–8 dominate all the eddy conversions in middle latitudes; 5) one of the four waves in the $n = 4$ *CE* conversion in the tropics coincides with the SPCZ, while the remaining three correspond to the continental areas of Africa, Australia and South America; and 6) during the last three days, when the SPCZ is decaying, the importance of the $n = 4$ contribution to *CE* is negligible.

1. Introduction

The Global Weather Experiment (GWE), also known as FGGE, provided an excellent opportunity to investigate global circulations based on observational data. This paper uses data taken during part of the first Special Observing Period (SOP-1) of the GWE to diagnose circulation features and their corresponding energy conversions in the Southern Hemisphere. In particular, it focuses on the period 10–27 January 1979 and investigates one of the major features present at that time—the South Pacific Convergence Zone (SPCZ).

In previous papers, Vincent (1982) and Huang and Vincent (1983) found that the SPCZ and its accompanying cloud band were quasi-stationary persistent features of the circulation from 10–18 January, that they propagated slowly westward and began to weaken slightly from 19–24 January and that they dissipated, except for their northernmost zonal portion (i.e., ITCZ), from 25–27 January (see Fig. 1 in Huang and Vincent, 1983). The present paper is an extension of their work and attempts to relate the circulation features of the SPCZ to those of the Southern Hemisphere. Streten (1973) and Trenberth (1976) among others have suggested that the SPCZ plays a significant role in the general circulation of the Southern Hemisphere.

Results are presented for four areas: the whole area, 0–60°S; the tropical sector, 0–30°S; the middle latitude sector, 30–60°S; and the portion of the tropical sector containing the most active part of the SPCZ, 0–30°S, 180–120°W. The study uses three approaches. First, since the SPCZ remained nearly stationary and reasonably active for the first 15 days of the analysis period (i.e., 10–24 January), 15-day time-averaged variables are shown to represent the mean state of the atmosphere. Rosen and Salstein (1982), in a study of the Northern Hemisphere wintertime circulation, suggested that averaging periods of at least ten days are necessary in order to separate zonal mean transient from standing eddy processes which occur on less than a seasonal time scale. The 15-day period used to compute the time-averaged quantities presented herein is taken to be representative of large-scale eddies which contribute to the general circulation. Second, in order to compare day-to-day variations of variables to their mean state as well as view the persistent nature of the SPCZ and its eventual demise, daily changes in the circulation patterns are examined for the entire 18-day

* Current affiliation: Atmospheric Science Program, University of North Carolina, Asheville, NC 28804.

period. Finally, a zonal wavenumber analysis of selected variables is presented so that the relative roles of mean and eddy motions and the significance of the location of the SPCZ within the general circulation pattern of the Southern Hemisphere can be pursued.

A detailed description of the data sources and computational procedures used in this paper is given by Vincent (1982) and will not be reiterated here. However, since that paper our data coverage has been expanded to include all of the Southern Hemisphere. As noted above, the present analysis encompasses all longitudes from 0–60°S. In brief, the data set consists of grid point values of geopotential height, temperature (derived hydrostatically from the height field), horizontal wind components and relative humidity, all at standard pressure levels from 1000–100 mb, and mean sea level pressure. These variables were reproduced, with some modifications (see Vincent, 1982), at increments of 2.5° lat/long from the original set of FGGE Level III-b analyses produced at the European Centre for Medium-Range Weather Forecasts (ECMWF). Due to the extensive areal coverage in this study, the grid increment was increased to 5° lat/long using a 9-point weighted smoothing scheme. Vertical motions, which represent an important part of the study, were calculated from the horizontal divergence of the analyzed winds using the kinematic method. An O'Brien (1970) mass adjustment scheme was applied in which the vertical motion, ω, was set to zero at 1000 and 100 mb. It is realized that ω does not necessarily vanish at these two levels, but the values are sufficiently small to justify the approximation for convenience. The lower boundary condition is reasonable in most locations since the grid spacing is five degrees, and most grid points do not involve topography. It is worth noting that the original ECMWF (initialized) values were found to be about a factor of three less than the recomputed values. In summary, the only variable in the data set that is not based on gridded analyzed variables is relative humidity, but it is not used in the present study.

2. Energy conversions

Since energy conversions form an integral part of this paper, some comments on the methods which were applied to obtain the conversions is warranted. Lorenz (1955) introduced a formulation of the energy equations in which he separated the mean and eddy (deviation from the mean) contributions of available potential energy (APE) and kinetic energy in order to study the large-scale atmospheric generation, dissipation and conversion of energy. Oort (1964) partitioned the total APE and kinetic energy into mean and eddy components using three different averaging techniques which he called space domain, time domain and mixed space–time domain. In the present study, only the space and mixed space–time domains are used. The definitions of the energy conversions in these domains, as well as a brief development of the spectral energy conversions terms, follows.

a. Space domain

The equations used here are similar to those of Oort (1964), Muench (1965) and Brennan and Vincent (1980). The latter reference provides a physical interpretation of terms. This set of equations is used to study the daily variations of energy conversions discussed in Section 3. The equations are:

$$CZ = -\frac{R}{g}\int \frac{[\omega]''[T]''}{p}\,dp,$$

$$CE = -\frac{R}{g}\int \frac{[\omega^*T^*]}{p}\,dp,$$

$$CA = -\int \frac{1}{\sigma}\left([v^*T^*]\frac{\partial[T]}{a\partial\phi} + [\omega^*T^*]\frac{\partial[T]''}{\partial p}\right)dp,$$

$$CK = \frac{1}{g}\int \left([u^*v^*]\cos\phi\,\frac{\partial}{a\partial\phi}\frac{[u]}{\cos\phi}\right)dp,$$

where σ is the stability parameter,

$$\sigma = \frac{gp}{R}\left\{\frac{R}{c_p}\frac{\tilde{T}}{p} - \frac{\partial\tilde{T}}{\partial p}\right\}.$$

A bracket denotes a zonal average, an asterisk a deviation from the zonal average and a tilde the area average of a variable over a pressure surface, i.e.,

$$(\tilde{\ }) = \frac{1}{(\lambda_e - \lambda_w)(\sin\phi_n - \sin\phi_s)} \times \int_{\lambda_w}^{\lambda_e}\int_{\phi_s}^{\phi_n}(\ )\cos\phi\,d\phi\,d\lambda;$$

a double prime denotes the deviation from this area average and the vertical integration is from 1000 to 100 mb. The variables in the equations have conventional meteorological meanings.

The upper left panel of Fig. 6 depicts how each of the energy conversions influences the energy cycle. The contents are *AZ*, the zonal APE; *AE*, the eddy APE; *KZ*, the zonal kinetic energy; and *KE*, the eddy kinetic energy. The affixes, SE and TE symbolize standing and transient eddies.

b. Mixed space-time domain

This method has been widely used by many investigators to study the general circulation and climate (e.g., Oort, 1964; Kidson *et al.*, 1969; Newell *et al.*, 1974). The energy conversions are:

$$\overline{CZ} = -\frac{R}{g}\int \frac{[\bar{\omega}]''[\bar{T}]''}{p}\,dp,$$

$$\overline{CE} = -\frac{R}{g}\int \frac{[\overline{\omega'T'}]}{p} + \frac{[\bar{\omega}^*\bar{T}^*]}{p}\,dp,$$

$$\overline{CA} = -\int \frac{1}{\sigma}\left\{([\overline{v'T'}] + [\bar{v}^*\bar{T}^*])\frac{\partial[\bar{T}]}{a\partial\phi} + ([\overline{\omega'T'}] + [\bar{\omega}^*\bar{T}^*])\frac{\partial[\bar{T}]''}{\partial p}\right\}dp,$$

$$\overline{CK} = \frac{1}{g}\int ([\overline{u'v'}] + [\bar{u}^*\bar{v}^*])\cos\phi\frac{\partial}{a\partial\phi}\frac{[\bar{u}]}{\cos\phi}dp,$$

where σ is computed as in the space domain except $\tilde{T}$ is substituted for $\bar{T}$. An overbar denotes a time average and a prime a deviation from the time average.

c. *Spectral energy conversions*

Atmospheric variables can be decomposed into their zonal average and wave components using a zonal Fourier analysis technique proposed by Saltzman (1957, 1970). The Fourier transform pair for harmonic analysis around latitude circles is:

$$f(\lambda, \phi, p, t) = \sum_{n=-\infty}^{\infty} F(n, \phi, p, t)e^{in\lambda},$$

$$F(n, \phi, p, t) = \frac{1}{2\pi}\int_0^{2\pi} f(\lambda, \phi, p, t)e^{-in\lambda}d\lambda,$$

where λ is longitude, ϕ is latitude, and n is wave number. The functions $f(\lambda)$ and $F(n)$ to be considered here are:

$$f(\lambda): uv\omega zT,$$

$$F(n): UVWZB.$$

In the present study, we have decomposed the atmospheric variables into their zonal harmonic wavenumber domains for $n = 0$ and $n = 1$–15. For example, a variable, α, may be represented as:

$$\alpha = \alpha_0 + \sum_{n=-15}^{15} \alpha_n e^{in\lambda}$$

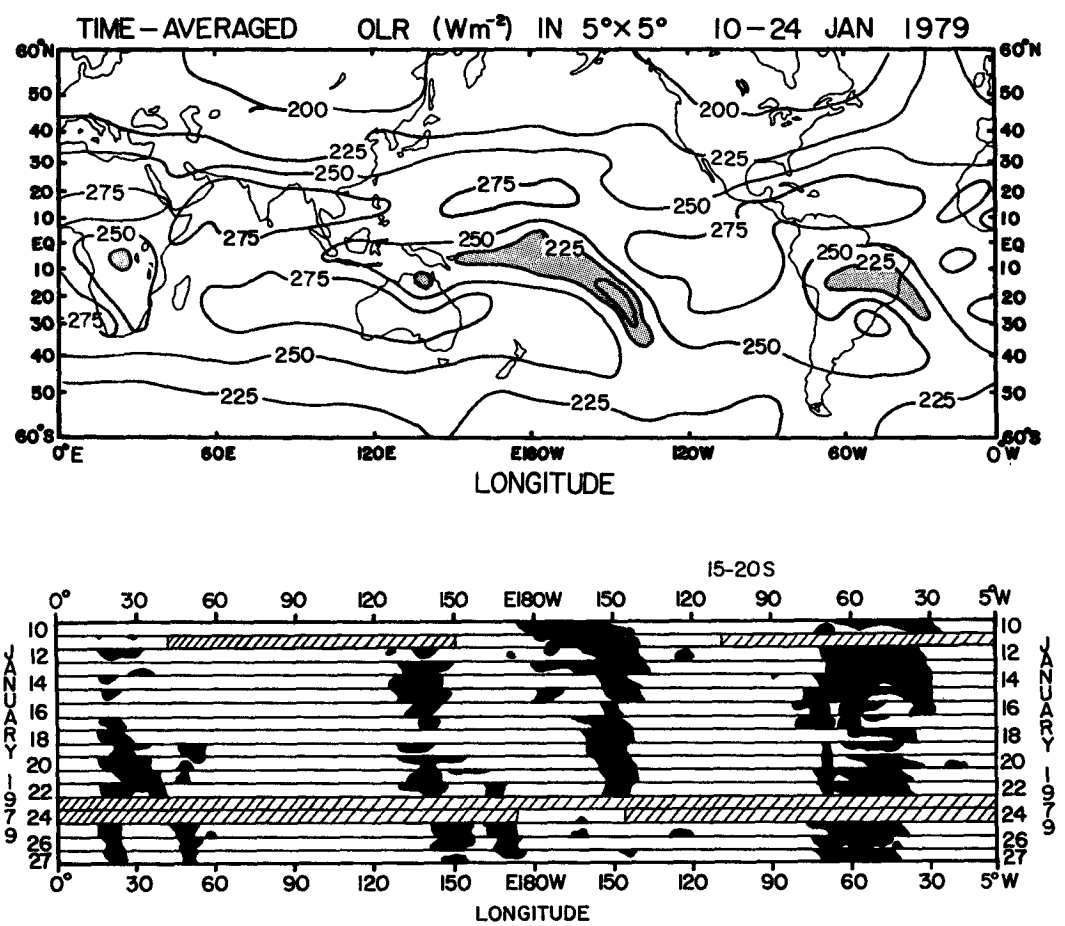

FIG. 1. Average outgoing longwave radiation (OLR) in W m^{-2} for 10–24 January 1979 (upper panel). Data for portions of 23–24 January were too sparse to use for analysis. The area $\leq$ 225 W m^{-2} is shaded to represent most likely deep convective activity in the tropics. Hovmöller diagram of OLR $\leq$ 225 W m^{-2} for latitude band of active convection, 15–20°S (lower panel).

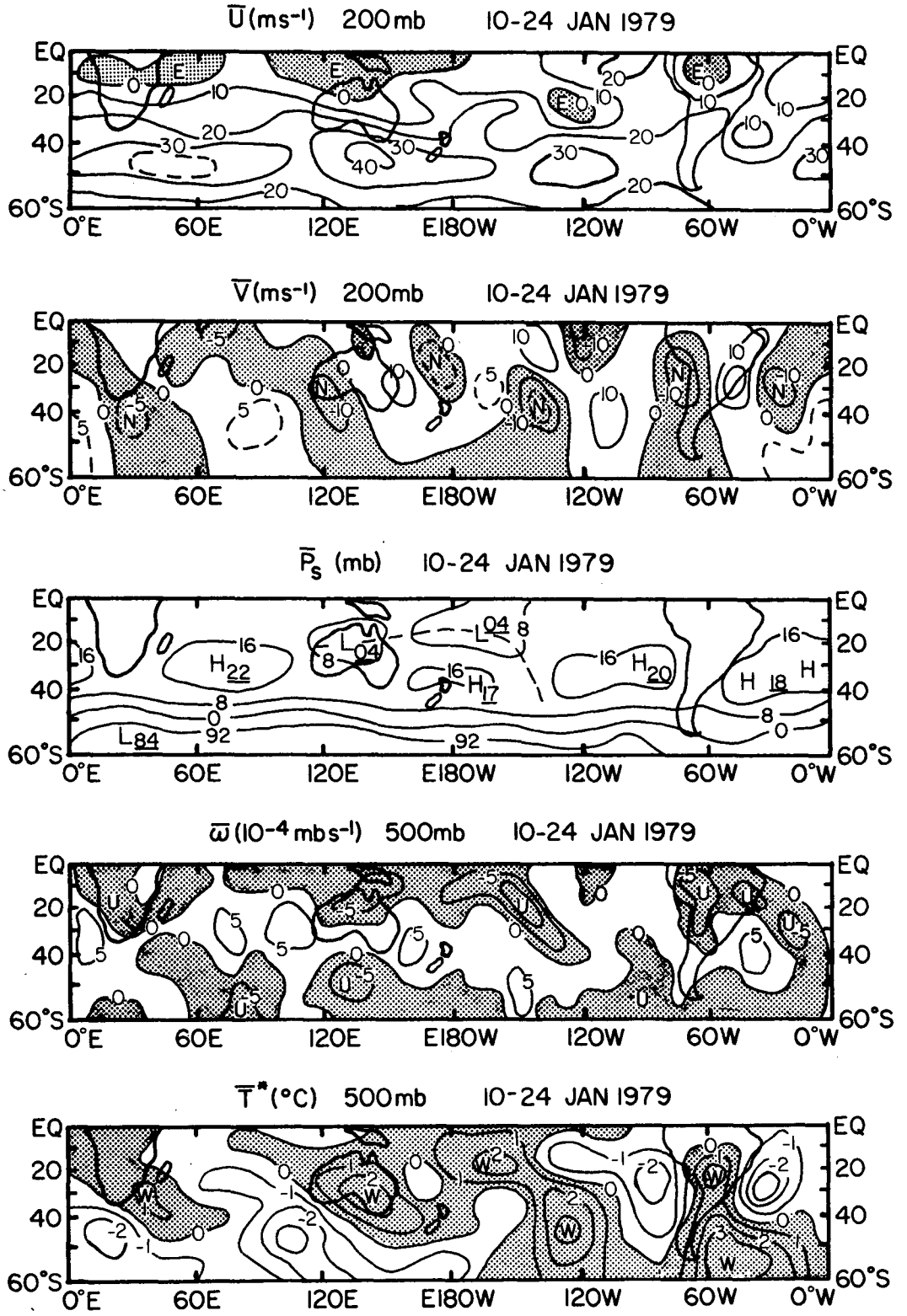

FIG. 2. Average zonal wind ($\bar{u}$) in m s^{-1} at 200 mb (top panel), meridional wind ($\bar{v}$) m s^{-1} at 200 mb (second panel), mean sea level pressure ($\bar{p}_s$) in mb (third panel), vertical p-velocity ($\bar{\omega}$) in 10^{-4} mb s^{-1} at 500 mb (fourth panel), and temperature anomaly ($\bar{T}^*$) in °C at 500 mb (bottom panel) for 10–24 January 1979. The temperature anomaly was computed by subtracting the zonally-averaged temperature at each 5° latitude band from the grid point values in that band.

where subscripts, 0 and n, denote the zonal average and a specific wavenumber, and α_n is a complex Fourier coefficient. It should be noted that $\alpha_0 = [\alpha]$, a zonally-averaged quantity.

The definitions of energy conversions in the spectral energy balance equations are similar to those of Saltzman (1970). They are:

$$CZ = -\frac{R}{g}\int \frac{[\omega]''[T]''}{p}\,dp,$$

$$CE(n) = -\frac{R}{g}\int \frac{[W(n)B(-n) + W(-n)B(n)]}{p}\,dp,$$

$$CA(n) = -\int \frac{1}{\sigma}\left\{[V(n)B(-n) + V(-n)B(n)]\frac{\partial[T]}{a\partial\phi} + [W(n)B(-n) + W(-n)B(n)]\frac{\partial[T]''}{\partial p}\right\}dp,$$

$$CK(n) = \frac{1}{g}\int \left\{[U(n)V(-n) + U(-n)V(n)]\frac{\cos\phi}{a}\frac{\partial}{\partial\phi}\frac{[u]}{\cos\phi}\right\}dp,$$

where σ is defined as that in the space domain equations.

Before proceeding to a discussion of results, it should be emphasized that this study considers only the conversion contributions to the energy cycle. There are several other contributions. Each of the areas examined is limited in horizontal and vertical extent. Hence, boundary transports can alter an individual area-averaged energy content. Also, each form of energy within an area can undergo changes due to *in situ* sources and/or sinks and local effects. Plumb (1983) has demonstrated that the physical interpretation associated with an individual component of the energy cycle needs to be considered with extreme caution. He suggests that the effects of both conversions and boundary transports are necessary for a proper interpretation of the complete energy cycle and he questions whether or not observational data are sufficiently accurate, in general, to compute energy budgets. He concludes that an energy budget approach may not be the best way to obtain a physical understanding of the atmospheric general circulation. We feel differently in that we believe the energy conversions do provide information which can be related to physical understanding of large-scale processes. In this paper, a variety of display techniques is used to illustrate the horizontal, vertical and temporal distributions and/or variations of each of the conversion terms. By representing the information in several forms, we hope to convince the reader of the significance of the SPCZ area with regard to certain segments of the energy cycle of the Southern Hemisphere, even though our discussion is restricted to energy conversions. Furthermore, where the results appear to warrant a physical explanation, we will attempt to offer one.

3. Results and discussion

Values of outgoing longwave radiation (OLR), derived from NOAA polar-orbiting satellites, were used to identify tropical convective activity. The radiation data were supplied to us by NESDIS/NOAA. Detailed explanations about radiation measurements produced

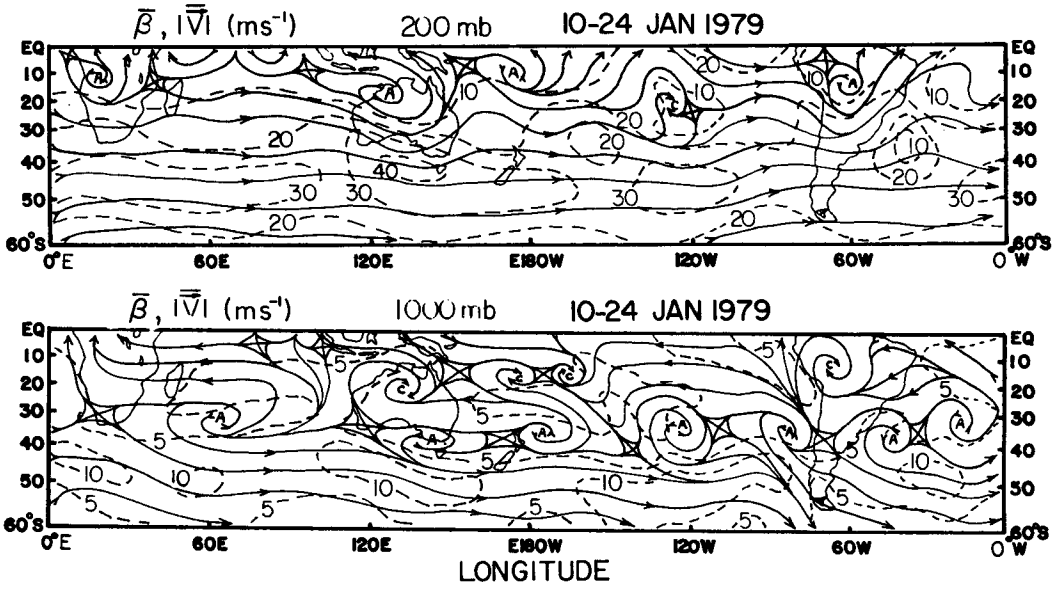

FIG. 3. Average streamlines and isotachs (m s^{-1}) at 200 mb (upper panel) and 1000 mb (lower panel) for 10–24 January 1979.

by NOAA satellites are given by Gruber and Winston (1978) and Winston *et al.* (1979). Figure 1 shows the time-averaged OLR for the period 10–24 January. The values for portions of 23 and 24 January were excluded from the average because of missing or insufficient data. The tropical areas occupied by values ≤ 225 W m^{-2} are shaded since they most likely contain deep convective activity a large percentage of the time (Heddinghaus and Krueger, 1981). The SPCZ and the cloud band over South America (hereafter referred to as SACZ) are the two dominant features in the tropics. However, over Africa and along the northern coast of Australia, convective cloud bands also are evident. In contrast to the other cloud systems, which appear to be tied to the three continents, the SPCZ is not near a large land mass. The notable protrusion of the SPCZ and the SACZ into midlatitudes implies that interactions are occurring between tropical and extratropical latitudes in these two regions. Figure 1 also shows the day-to-day changes in the areas occupied by values of OLR ≤ 225 W m^{-2} for the latitude strip 15–20°S. The persistence of the convective cloud bands over the three continents and SPCZ is quite striking. The cloud distribution suggests that there are three or four persistent convective areas in the tropics. We shall return to this point later in the discussion.

a. Large-scale circulation

Figure 2 shows horizontal distributions of time-averaged variables which depict the large-scale circulation features that were present during 10–24 January. The horizontal wind components at 200 mb illustrate that wave motion is present and that cross-equatorial flow between the Northern and Southern Hemispheres can be significant. Two locations where maximum flow into the Northern Hemisphere takes place are north of the northern boundaries of the SPCZ and SACZ (also see Fig. 3). The zonal wind component is dominated by westerly flow with maximum values near 45°S. The surface pressure pattern clearly indicates the summertime subtropical high pressure belt. Also evident is a low pressure trough which extends from Australia eastward to the South Pacific and then southeastward. This is tied to the thermal low over western Australia, the monsoon circulation over northern Australia and Indonesia, the ITCZ and the SPCZ. Cyclonic systems frequently form over the Pacific Ocean and propagate eastward and southeastward along this trough. During the period examined, three cyclones, behaving in this manner, were observed in the vicinity of the SPCZ (Vincent, 1985). The remaining two panels in Fig. 2 show that, in general, relatively warm (cold) air is rising (sinking) in the middle troposphere. This type of thermally-direct circulation, which is responsible for a conversion of eddy available potential energy to eddy kinetic energy (i.e., $CE > 0$), is particularly strong in the area occupied by the SPCZ. More will be said later concerning this point.

Figure 3 shows the 1000 and 200 mb time-averaged streamline and isotach patterns. At 1000 mb, the two prominent features are 1) the series of anticyclones near 35°S that are associated with the subtropical high pressure belt and 2) the series of cyclones stretching from Australia to the South Pacific that are associated with the monsoonal trough and the SPCZ. At 200 mb, the

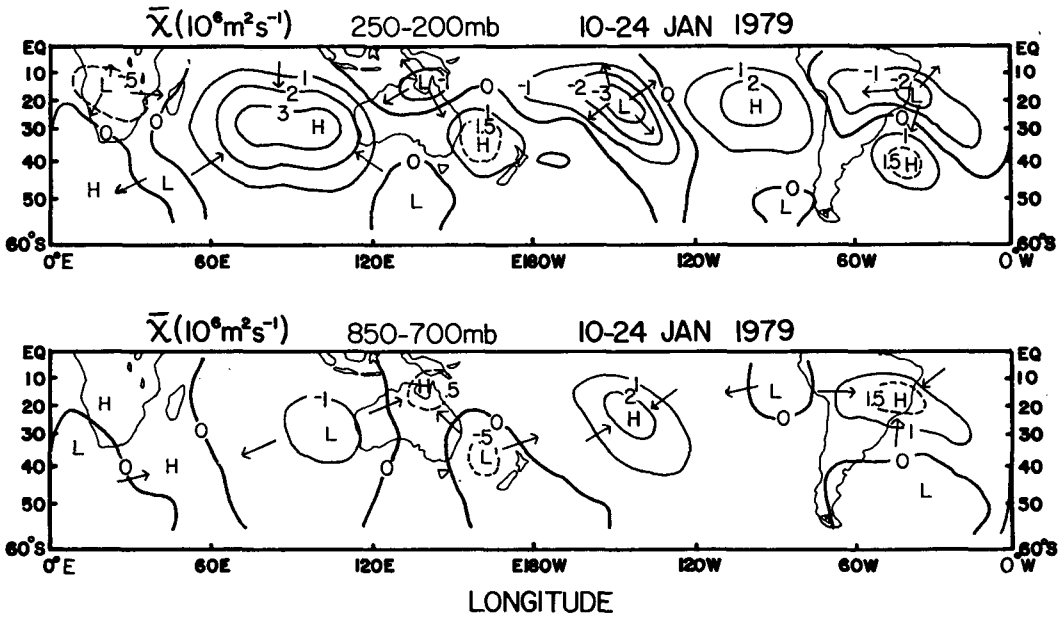

FIG. 4. Average velocity potential ($\bar{\chi}$) in 10^6 m^2 s^{-1} in 250–200 mb layer (upper panel) and 850–700 mb layer (lower panel) for 10–24 January 1979. Arrows indicate direction of the divergent wind.

salient features are the westerly jet stream near 45°S, the previously mentioned cross-equational flow, and a local subtropical jet, oriented northwest–southeast, in the vicinity of the SPCZ. The latter feature plays an important role in the local baroclinicity associated with cyclonic activity along the SPCZ during this period (Vincent, 1985).

A useful variable for depicting many of the features cited above is the velocity potential. Figure 4 shows distributions of velocity potential, together with the divergent component of the wind for the 850–700 mb and 250–200 mb layers. Each of the major convective regions depicted in Fig. 1 shows low-level convergence and upper-level divergence. In particular, note that the SPCZ is embedded in one of the strongest convergent–divergent areas. Also note that upper level cross-equatorial flow is occurring north of the SPCZ.

Several time-averaged variables have been displayed which suggest that the SPCZ is a dominant feature of the mean-state Southern Hemisphere circulation dur-

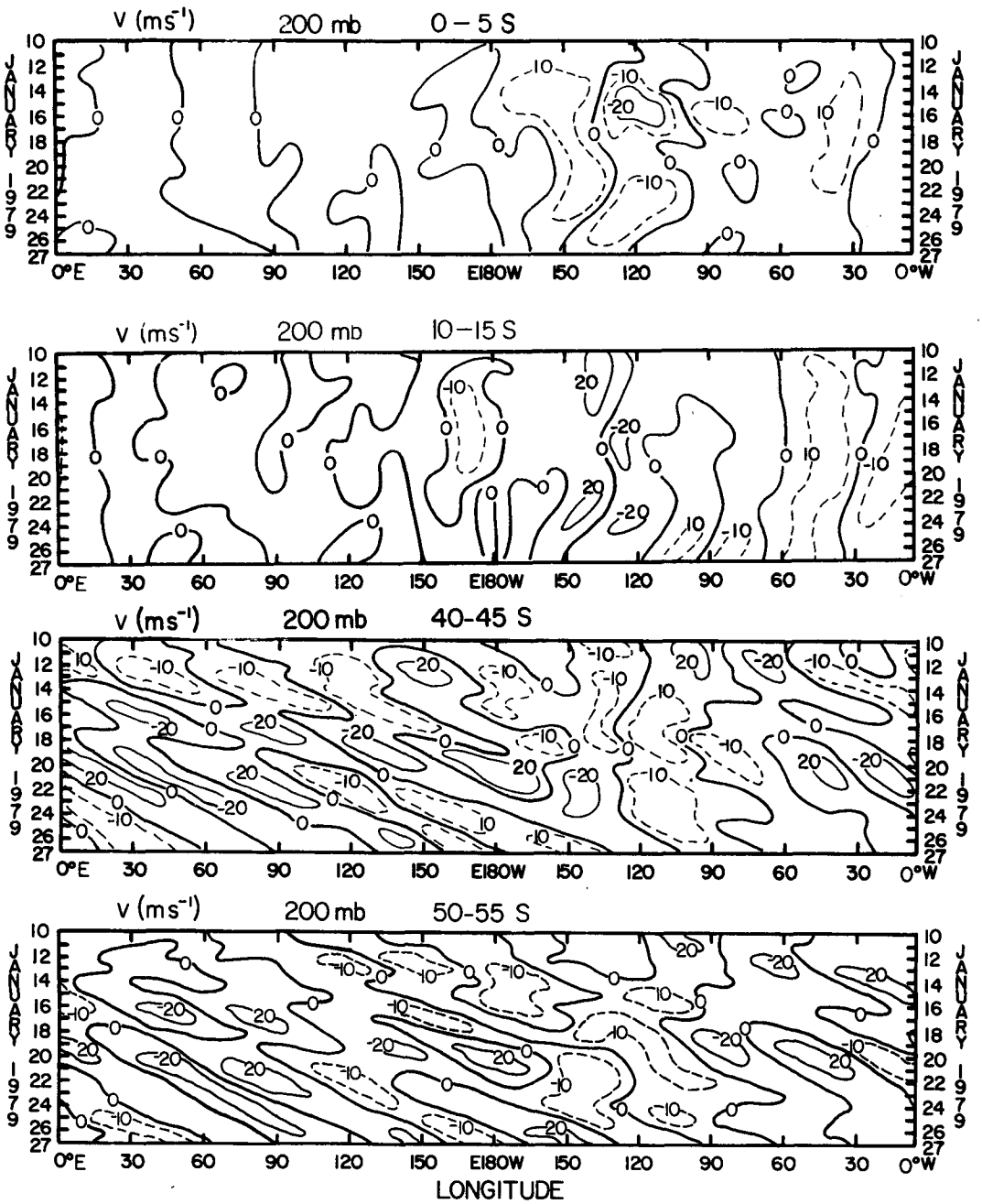

FIG. 5. Hovmöller diagrams of the south–north component of wind v at 200 mb (m s^{-1}) for latitude bands 0–5°S, 10–15°S, 40–45°S and 50–55°S during 10–27 January 1979.

ing the period examined. However, except for the convective cloud depictions given in Fig. 1, day-to-day variations have not yet been explored. A convenient chart for depicting daily changes, as well as providing an indication of wave activity (which is an important aspect of Section 3b) is the Hovmöller diagram. Figure 5 shows such a diagram for the meridional component of the wind at 200 mb for latitude bands 0–5°S, 10–15°S, 40–45°S and 50–55°S. The 0–5°S diagram shows that significant cross-equatorial flow occurs north and northeast of the SPCZ throughout the period. The diagram for the 10–15°S latitude band, which contains the SPCZ, shows the quasi-stationary nature of the circulation over the SPCZ and SACZ. In general, the wind is northerly over the convective regions (see Fig. 1) and southerly on either side. In middle latitudes, it is clear that transient waves are propagating eastward and it appears that wavenumber 5 is important. One exception to this pattern occurs in the vicinity of the SPCZ, which has its southern tip near 40–45°S, between 130°W and 140°W prior to its dissipation. The 40–45°S diagram shows a quasi-stationary wave associated with the SPCZ during its active phase from 10–24 January. However, the diagram for 50–55°S, which is south of the SPCZ, shows that transient waves occur at all longitudes. Thus, the SPCZ seems to act as a barrier to (or absorber of) the traveling waves in that they do not continue their eastward propagation in its vicinity.

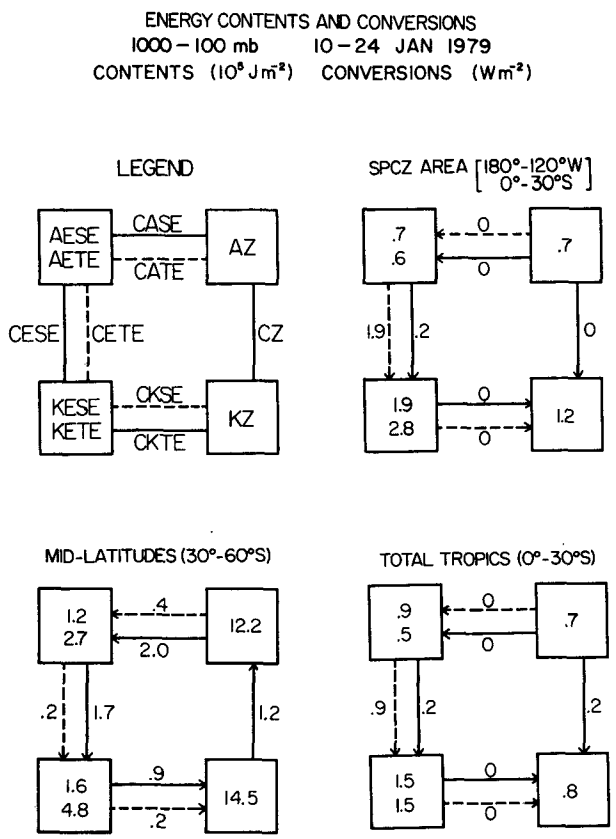

FIG. 6. Average energy contents and conversions for 0–30°S, 30–60°S and 180–120°W, 0–30°S for period 10–24 January 1979. Values are vertically-integrated and area-averaged, with contents in 10^5 J m^{-2} and conversions in W m^{-2}. SE and TE suffixes stand for standing and transient eddy components.

TABLE 1. Energy conversions from $AZ \rightarrow AE$ (CA), $AE \rightarrow KE$ (CE) and $KE \rightarrow KZ$ (CK) in W m^{-2}.

Conversion	Present study 10–24 Jan 79 0–60°S	Newell *et al.* (1974) Dec–Feb 0–90°S	Kung and Tanaka (1983)* FGGE: SOP-1 90°N–90°S
CA	0.9	0.9	2.0
CE	1.4	not given	2.1
CK	0.6	0.3	0.6

* Based on ECMWF data.

b. *Energy conversions*

Energy conversions in mixed space–time domain are presented in Fig. 6 for the total tropics, the SPCZ portion of the tropics and for middle latitudes. Contents are presented also, but are not discussed. Before discussing the results it is worth noting again that there are several ways in which the content of a particular type of energy can be altered. Of these, the conversion terms are believed to be the most reliable of the complete energy budget terms. Sources and sinks due to generation and dissipation generally depend on either parameterization techniques or residual computations, while boundary transports, particularly for potential energy, are difficult to assess accurately. The conversion terms, however, contain the effects of the zonally-symmetric and asymmetric (wave) portions of the mass and motion fields and involve momentum and heat transports. Therefore, they give a good representation and physical understanding of the circulation features that are present.

In Fig. 6, the only significant conversion term in the total tropics is CE, which shows that thermally-direct eddy circulations are dominant there. Moreover, the major contribution to CE is by the standing eddies. In midlatitudes the values of conversion terms are generally much greater than their tropical counterparts and transient eddy contributions dominate. All conversion terms are the same order of magnitude and appear to make important contributions to the midlatitude energy budget. In the SPCZ area, as for the total tropics, the only significant conversion term is CE. Its value is about twice that in the tropics, with the standing eddy contribution dominating, suggesting that the SPCZ, which was a quasi-stationary feature during this period, plays an important role in the eddy kinetic energy production in the tropical Southern Hemisphere.

It is interesting to compare the present conversion

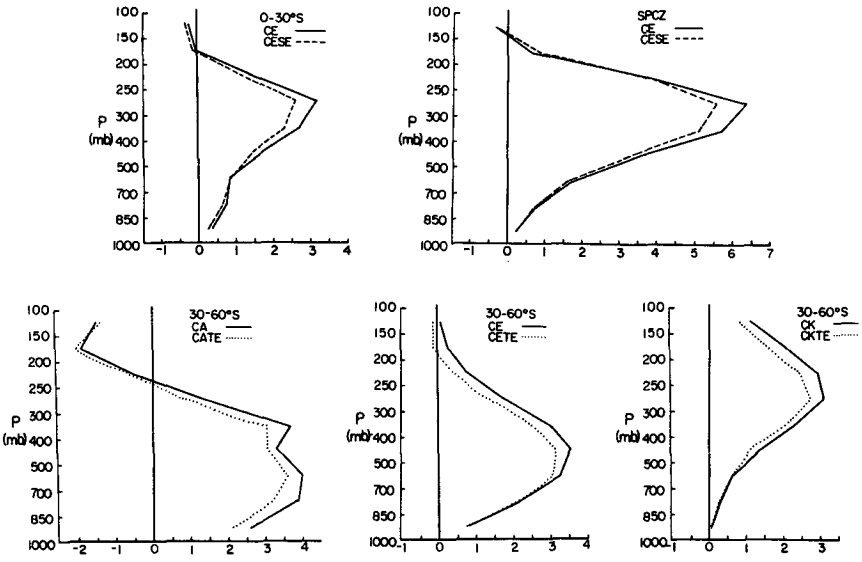

FIG. 7. Vertical distributions of area-averaged energy conversions in 10^{-4} W kg^{-1} for selected areas for 10–24 January 1979.

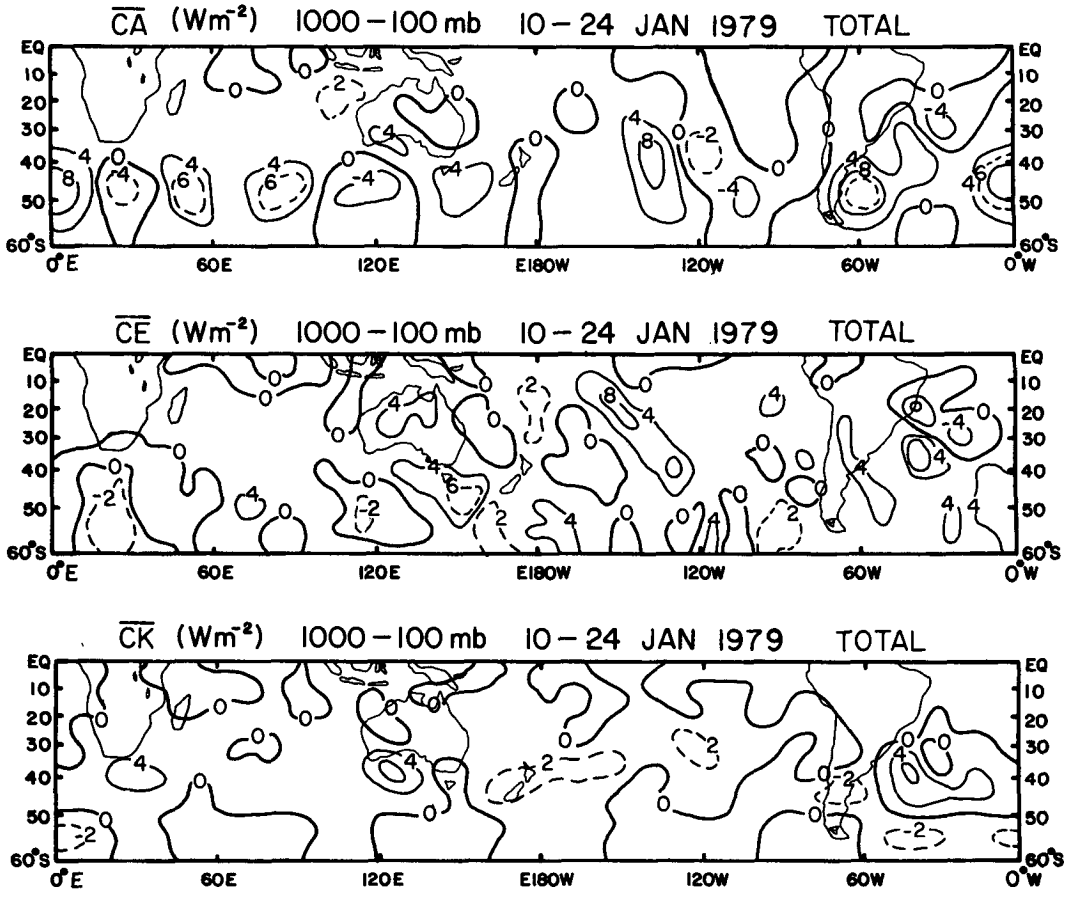

FIG. 8. Charts of time-averaged vertically-integrated energy conversions, *CA* (upper panel), *CE* (middle panel) and *CK* (lower panel) in W m^{-2} for 10–24 January 1979.

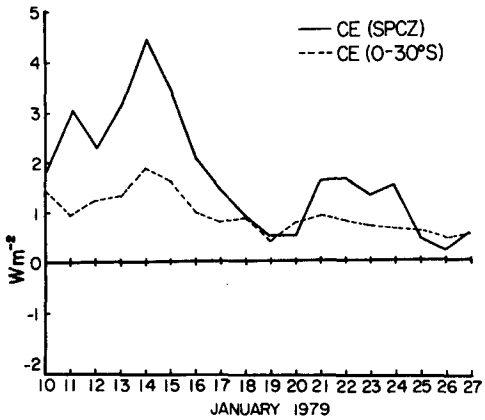

FIG. 9. Time series of vertically-integrated, area-averaged values of *CE* conversion in W m^{-2} for the SPCZ area and 0–30°S during 10–27 January 1979.

rates for 0–60°S to those of Newell *et al.* (1974) for December–February, 0–90°S, and Kung and Tanaka (1983) for SOP-1, 90°N–90°S. In the first reference the area is more representative to that presently used, while in the latter reference the time period is more representative. Table 1 shows the comparison. It is seen that the results of the three studies are in total agreement with regard to signs of individual terms and that the magnitudes are within a factor of two of each other. The results of Kung and Tanaka include the northern wintertime circulation which presumably is the reason for their larger values of *CA* and *CE*.

Figures 7 and 8 depict vertical and horizontal distributions of the energy conversions. Figure 7 shows vertical profiles of *CE* for the total tropics and SPCZ areas, as well as profiles of *CA*, *CE* and *CK* for the midlatitude area. The figure reveals that the standing (transient) eddy component of *CE* (*CA*, *CE*, *CK*) dominates at all levels in the tropics (middle latitudes). Figure 8 shows horizontal distributions of vertically-integrated values of *CA*, *CE* and *CK* and verifies that one of the most important areas contributing to the conversion from *AE* to *KE* is the SPCZ. The figure also shows evidence of middle latitude wave activity through the alternating signs of the conversion terms, particularly *CA*.

In Fig. 6 it was seen that the time-averaged value of *CE* in the SPCZ area was about two times greater than for the total tropics. The day-to-day changes of *CE* for these two regions are compared in Fig. 9. Since temporal variations are now involved, the space–time domain equations given in Section 2 can no longer be used. Instead, the space domain equations are used. Thus, the partitioning of a variable now consists of a zonal average and a deviation from the zonal average (eddy component). Figure 9 shows that the trend of *CE* in the two regions is similar, but that individual values in the SPCZ are about twice as large as the respective values in the total tropics. Thus, on a daily basis, as well as on a time-averaged basis, the SPCZ plays a significant role in this baroclinic conversion term. Values peak on 14 January and then decrease for several days before showing a slight increase again during 21–24 January. It is interesting to note that after 24 January *CE* decreases to its lowest value. A similar trend was found in the eddy kinetic energy content, *KE*, for the SPCZ area (not shown). It decreased by a factor of two from 25–27 January. Recall that the latter period corresponds to the demise of the SPCZ (e.g., see lower panel, Fig. 1). Hence, there appears to be a good correlation between a high (low) level of energy and an active (inactive) SPCZ in the South Pacific.

It was noted earlier that three or four active convection areas persisted in the tropics throughout the period, except for the SPCZ after 24 January (see Fig. 1). Because of the persistence of this convective activity and the strong possibility that $CE > 0$ depends, at least in part, on the effects of moist convection and latent heat release (i.e., warmer air rising, colder air sinking), an analysis of the time-averaged variables that correspond favorably to convection and *CE* was performed. These variables are temperature anomalies at 500 mb, vertical *p*-velocities at 500 mb and geopotential height at 200 mb. The physical reasoning for selecting these variables is that warm air rising in the middle troposphere should cause an inflation of the upper-level height field, whereas cold air sinking would be commensurate with lower heights. A typical example of the resulting analysis for the tropics is shown in Fig. 10 for the latitude band 20–25°S. This band contains the SPCZ, as well as the continents of Africa, Australia

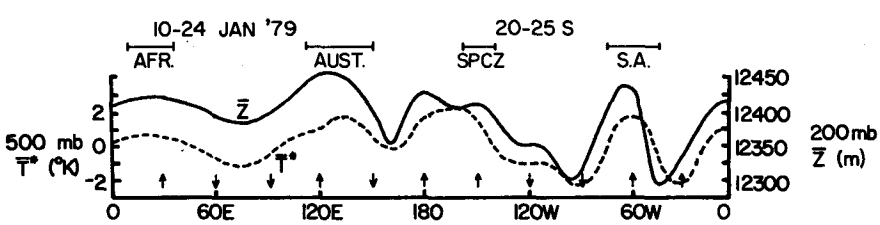

FIG. 10. Time-averaged longitudinal distribution of geopotential height ($\bar{z}$) at 200 mb in m (solid line) and temperature anomaly ($\bar{T}^*$) at 500 mb in K (dashed line) for latitude band 20–25°S for 10–24 January 1979. Arrows at bottom indicate direction of vertical *p*-velocity ($\bar{\omega}$) at 500 mb.

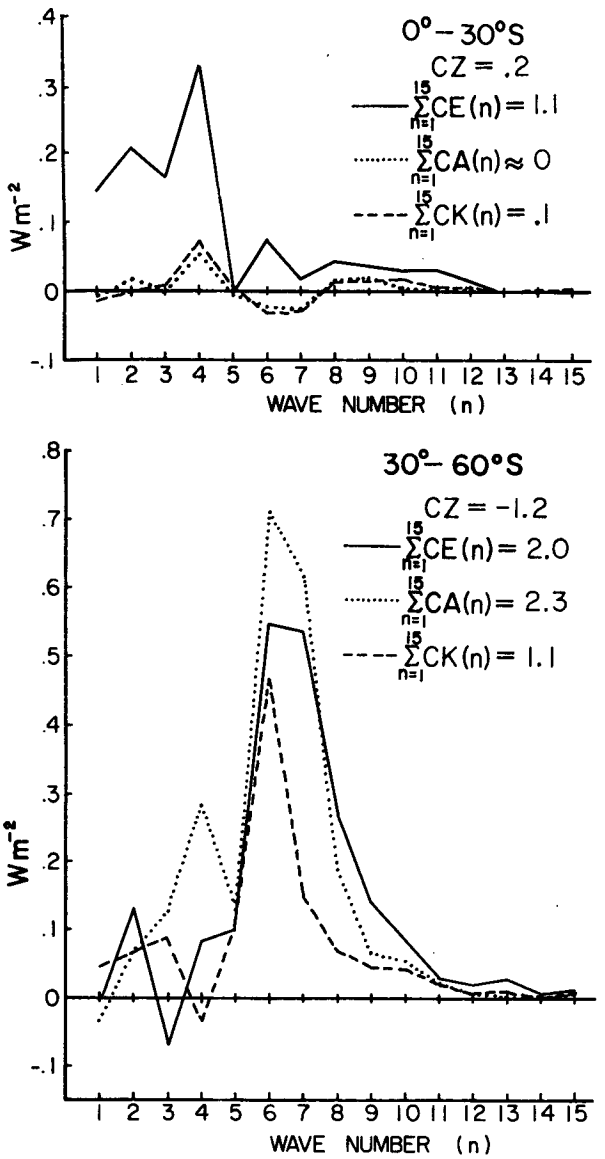

FIG. 11. Spectral diagrams of vertical integrals of time and area-averaged energy conversions in W m^{-2} for 0–30°S and 30–60°S for period 10–24 January 1979.

and South America. The figure shows that rising warm air and sinking cold air at midlevels occur in conjunction with higher and lower heights, respectively, at 200 mb. Furthermore, it is seen that four warm ridges exist and that they are located over the three continents and the SPCZ. Although the geographical spacing between each of the ridges is not precisely 90 degrees, it is sufficiently close to suggest that wavenumber 4 may make an important contribution to *CE* for this latitude band. A perusal of other five degree latitude bands in the tropics revealed a similar wave structure between 15 and 30°S, but not beyond these latitudes. Since the three continents and the SPCZ are located within these latitude limits, and *all* four of them do not extend outside these latitudes, it appears that the land masses and the SPCZ have a major impact on the wave activity. In order to quantitatively assess the significance of wavenumber 4 in the tropics with regard to *CE* and other conversion terms, as well as identify the locations where troughs and ridges for each wavenumber (n) occur, a spectral analysis of the data was performed. The method applied, which was described in Section 2, uses the space domain approach and takes into account the zonal average (i.e., $n = 0$) and deviations from the zonal average ($n = 1$–15). Therefore, the time-averaged energy conversions presented in this discussion may be slightly different from those presented earlier (i.e., derived from the mixed space–time domain approach) due to contributions from $n > 15$.

Figure 11 shows the time mean and area-averaged conversions for the total tropics and for middle latitudes during 10–24 January. It should be noted that these and all subsequent spectra are discrete line-spectra and hence, are meaningful only for the integral values of wavenumber. To aid visually in tracing the fluctuations of the spectra, however, lines have been drawn between points on the diagrams. The summation of each eddy quantity from $n = 1$–15 and its zonal average ($n = 0$) are also given.

The values of all conversions are in good agreement, both in the tropics and midlatitudes, with those derived in mixed space–time domain (compare Fig. 11 to Fig. 6). In the tropics, Fig. 11 shows that $n = 4$ makes the main contribution to $CE(n)$, whereas the other two eddy conversion terms are small at all wavenumbers. The value of $CE(n)$ at $n = 4$ accounts for about 30% of the total energy conversion, *CE*. Remarkable contrasts in the wavenumber domain are found between the tropics and midlatitudes. The conversions in midlatitudes are dominated by synoptic-scale waves ($n = 5$–8), and have greater magnitudes than those in the tropics. It is interesting to note that Kung and Tanaka (1983) also found large $KE(n)$ at $n = 5$ and 6, in ad-

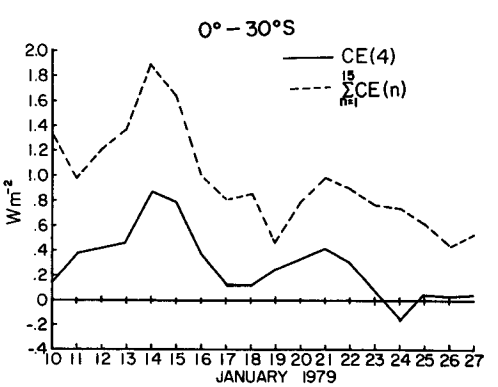

FIG. 12. Time series of vertically-integrated, area-averaged values of *CE* conversion in W m^{-2} for $n = 4$ and for the sum of all wavenumbers $n = 1$–15, for 0–30°S during 10–27 January 1979.

dition to $n = 1$, in the middle latitude Southern Hemisphere during SOP-1. The peaks of $CE(n)$ at $n = 6$ and 7 correspond roughly to the most unstable wavelengths predicted by the theory of baroclinic instability in the extratropics (Kuo, 1952).

Because of the importance of $n = 4$ in the CE conversion in the tropics, and the emphasis in this paper on the significance of the SPCZ in the energy conversions of the tropics, daily variations of $CE(n)$ are shown for $n = 4$ and for the sum of all waves $n = 1$–15 (Fig. 12). It is seen that for most of the period from 11–22 January, the contribution by $n = 4$ to the total value of $CE(n)$ is between 30 and 50%. After 22 January, when the SPCZ begins to weaken and dissipate, the $n = 4$ contribution is negligible.

Since $n = 4$ plays an important role in the CE conversion in the tropics and it is physically related to $\bar{\omega}$ and $\bar{T}^*$ in the middle troposphere and $\bar{z}$ in the upper troposphere, it is worthwhile to see how the ridge-trough positions of these variables relate to one another. Figure 13 shows the locations of the 200 mb height ridges, 500 mb thermal ridges and 500 mb maximum upward motion axes for $n = 4$, as well as the locations of the most active convective regions (i.e., OLR $\leq$ 225 W m^{-2}). The three variables are well correlated, as expected. Also, as expected, three of the four waves are tied to the continents of South America, Africa and Australia, whereas the fourth wave occurs over the open sea and coincides extremely well with the SPCZ.

One might be tempted to say that the SPCZ positioning of wavenumber 4 in these variables is nothing more than an artifact of its location relative to the three continents. The natural question that arises is: Are the three variables, and thus the CE conversion, significant in the SPCZ area because of *in situ* physical and dynamical processes or because of mechanical forcing due to the presence of the continents? In a diagnostic study such as the present one this question cannot be answered directly. Nevertheless, we have established that the SPCZ makes an important contribution to the

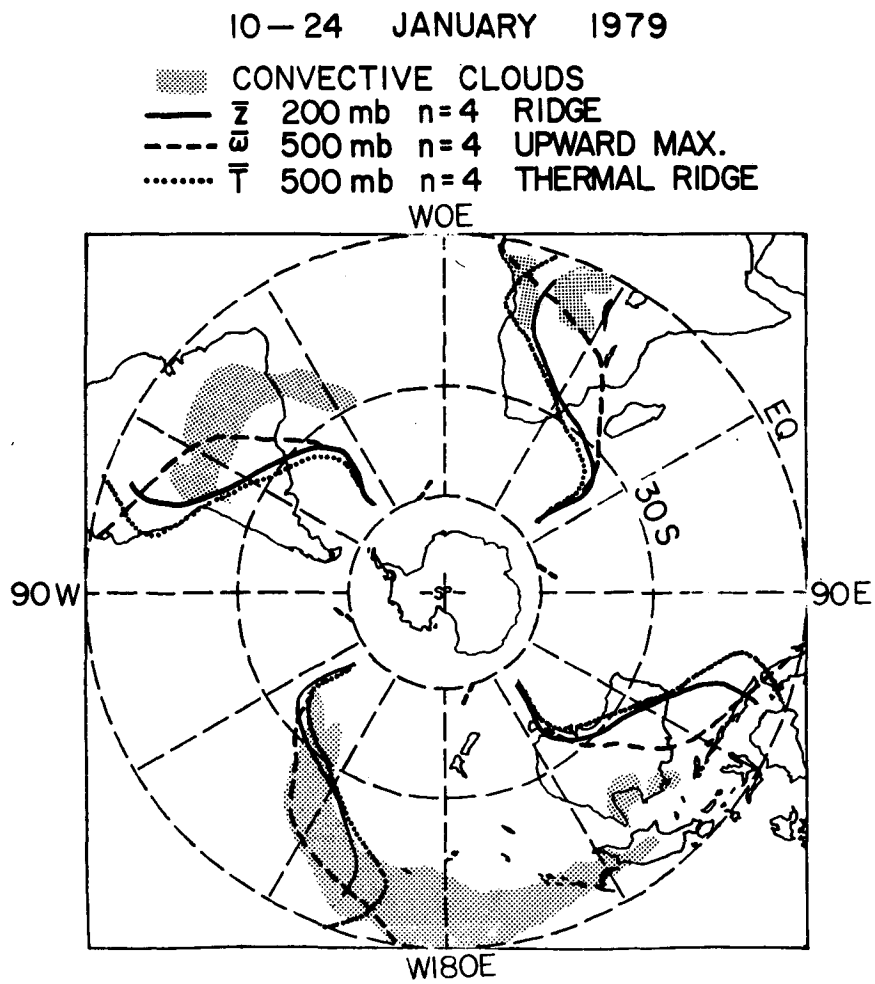

FIG. 13. Locations of 200 mb $\bar{z}$ ridges, 500 mb $\bar{\omega}$ axes of maximum upward motion and 500 mb T thermal ridges for wavenumber 4. The shaded portions represent deep convective cloud activity as in Fig. 1.

CE conversion for the total tropics during the period studied and that wavenumber 4 dominates over other wavenumbers in the tropics when the SPCZ is active. We pursued this point further by comparing our results of *CE* for $n = 4$ for 0–30°S with those we computed using the GFDL and ECMWF analyses presented by Kung and Tanaka (1983, 1984). It appears that our value of 0.35 W m^{-2}, derived for the period 10–24 January, is approximately twice as large as their ECMWF value for all of SOP-1. The SPCZ was active during our period of study, but was relatively inactive (based on satellite IR imagery) throughout the remainder of SOP-1.

4. Concluding remarks

Since the SPCZ is known to be a major circulation feature in the Southern Hemisphere throughout most of the year, our findings may contain an important message for operational forecasters and numerical modelers whose interests lie in medium and long-range prediction in the Southern Hemisphere tropics. First of all, we have established that during the period 10–24 January 1979, when the SPCZ was convectively active, it played a significant role in the baroclinic energy conversion *CE* within the tropical Southern Hemisphere. When the SPCZ dissipated the *CE* conversion did likewise. Second, our zonal wavenumber analysis showed that wavenumber 4 was dominant in the *CE* conversion process in the Southern Hemisphere tropics when the SPCZ was active, but that it did not dominate when the SPCZ dissipated. Third, we illustrated that the most intense convective activity in the tropics occurred in the SPCZ and that its location corresponded favorably to maximum values of $CE > 0$. Thus, it appears that the baroclinic process of warm air rising and cold air sinking in the large-scale waves of the tropical Southern Hemisphere is an important one and, furthermore, that an active SPCZ associated with wavenumber 4 makes a significant contribution to this process.

Acknowledgments. The authors thank Drs. Julia Paegle and John Ward for their assistance in supplying them with the ECMWF data. They also thank Dr. Phillip J. Smith and Mr. Ching-Chi Wu for their scientific discussions and the reviewers for suggestions which greatly improved the manuscript. Also, they appreciate the help provided by Mr. Douglas Miller who drafted the figures and Ms. Helen Henry who typed the manuscript. The research was sponsored by the Global Atmospheric Research Program, Division of Atmospheric Science, National Science Foundation and the National Oceanic and Atmospheric Administration under Grant ATM 82-00684 and by the National Aeronautics and Space Administration under Contract NAS8-35187.

REFERENCES

Brennan, F. E., and D. G. Vincent, 1980: Zonal and eddy components of the synoptic-scale energy budget during intensification of Hurricane Carmen (1974). *Mon. Wea. Rev.*, **108,** 954–965.

Gruber, A., and J. A. Winston, 1978: Earth–atmosphere radiative heating based on NOAA scanning radiometer measurements. *Bull. Amer. Meteor. Soc.*, **59,** 1570–1578.

Heddinghaus, T. R., and A. F. Krueger, 1981: Annual and interannual variations in outgoing longwave radiation over the tropics. *Mon. Wea. Rev.*, **109,** 1208–1218.

Huang, H.-J., and D. G. Vincent, 1983: Major changes in circulation features over the South Pacific during FGGE, 10–27 January 1979. *Mon. Wea. Rev.*, **111,** 1611–1618.

Kidson, J. W., D. G. Vincent and R. E. Newell, 1969: Observational studies of the general circulation of the tropics: Long term mean values. *Quart. J. Roy. Meteor. Soc.*, **95,** 258–287.

Kung, E. C., and H. Tanaka, 1983: Energetics analysis of the global circulation during the special observation periods of FGGE. *J. Atmos. Sci.*, **40,** 2575–2592.

——, and ——, 1984: Spectral characteristics and meridional variations of energy transformations during the first and second special observations periods of FGGE. *J. Atmos. Sci.*, **41,** 1836–1849.

Kuo, H.-L., 1952: Three-dimensional disturbances in a baroclinic zonal current. *J. Meteor.*, **9,** 260–278.

Lorenz, E. N., 1955: Available potential energy and the maintenance of the general circulation. *Tellus,* **7,** 157–167.

Muench, H. S., 1965: On the dynamics of the wintertime stratosphere circulation. *J. Atmos. Sci.*, **22,** 349–360.

Newell, R. E., J. W. Kidson, D. G. Vincent and G. J. Boer, 1974: *The General Circulation of the Tropical Atmosphere and Interactions with Extratropical Latitudes, Vol. 2.* MIT Press, 370 pp.

O'Brien, J. J., 1970: Alternative solutions to the classical vertical velocity problem. *J. Appl. Meteor.*, **9,** 197–203.

Oort, A. H., 1964: On the energetics of the atmospheric energy cycle. *Mon. Wea. Rev.*, **92,** 483–493.

Plumb, R. A., 1983: A new look at the energy cycle. *J. Atmos. Sci.*, **40,** 1669–1688.

Rosen, R. D., and D. A. Salstein, 1982: General circulation statistics on short time scales. *Mon. Wea. Rev.*, **110,** 683–698.

Saltzman, B., 1957: Equations governing the energetics of the larger scales of atmospheric turbulence in the domain of wavenumber. *J. Meteor.*, **14,** 513–523.

——, 1970: Large-scale atmospheric energetics of the wavenumber domain. *Rev. Geophys. Space Phys.*, **8,** 289–302.

Streten, N. A., 1973: Some characteristics of satellite-observed bands of persistent cloudiness over the Southern Hemisphere. *Mon. Wea. Rev.*, **101,** 486–495.

Trenberth, K. E., 1976: Spatial and temporal variations of the Southern Oscillation. *Quart. J. Roy. Meteor. Soc.*, **102,** 639–653.

Vincent, D. G., 1982: Circulation features over the South Pacific during 10–18 January 1979. *Mon. Wea. Rev.*, **110,** 981–993.

——, 1985: Cyclone development in the South Pacific convergence zone during FGGE, 10–17 January 1979. *Quart. J. Roy. Meteor. Soc.*, **111,** 155–172.

Winston, J. A., A. Gruber, T. I. Gray, Jr., M. S. Varnadore, C. L. Earnest and L. P. Mannello, 1979: *Earth-Atmosphere Radiation Budget Analyses Derived from NOAA Satellite Data June 1974–February 1978, Vol. 1.* NOAA, 373 pp.